Structural features of a water-soluble arabinoxylan from the endosperm of wheat

Rainer A. Hoffmann, Johannis P. Kamerling, and Johannes F. G. Vliegenthart*

Bijvoet Center, Department of Bio-Organic Chemistry, Utrecht University, P.O. Box 80.075, NL-3508 TB Utrecht (The Netherlands)

(Received August 1st, 1991; accepted September 26th, 1991)

ABSTRACT

A cold-water-soluble wheat-endosperm arabinoxylan consisting of a backbone of (1→4)-linked β-D-xylopyranosyl residues that are variously unsubstituted, and 3- or 2,3-substituted with single α-L-arabinofuranosyl groups, was subjected to ^{1}H-n.m.r. spectroscopy. The results of 2D homonuclear Hartmann–Hahn and 1D ^{1}H-n.m.r. spectroscopy allowed the identification of 3- and 2,3-substituted xylose residues, each with adjacent unsubstituted xylose residues, and also substituted xylose residues with a substituted xylose residue as a neighbour. The ^{1}H-n.m.r. data were correlated with ^{13}C-n.m.r. data by means of a ^{13}C–^{1}H 2D proton-detected heteronuclear multiple-quantum correlation experiment, which showed that only different types of branching (*i.e.*, 3- and 2,3-) can be identified by the ^{13}C-n.m.r. data.

INTRODUCTION

Arabinoxylans, which are major components of the cell walls of cereal plants, have significant influences on the behaviour of the grain during milling[1], the quality of the flour[2], the rheological properties of the dough[3], and the quality of the bread[4]. Studies[5-7] of the structures of these polysaccharides have involved monosaccharide analysis, methylation analysis, and Smith degradation, and have revealed an overall pattern of substitution of the (1→4)-linked xylan backbone by arabinofuranosyl side chains. In order to understand the relation between structure and physical properties, the distribution of the arabinofuranose residues along the backbone must be determined. In this context, we now report the application of ^{1}H- and ^{13}C-n.m.r. spectroscopy, including 2D homonuclear Hartmann–Hahn (HOHAHA) and 2D proton-detected heteronuclear multiple-quantum correlation (HMQC) measurements, together with reference ^{1}H-n.m.r. data for enzymically generated arabinoxylan oligosaccharides[8,9], to a water-soluble wheat-endosperm arabinoxylan.

EXPERIMENTAL

General. — The arabinoxylan (WPAX$_{51B}$) was isolated[6] from the cold-water-soluble fraction of the white flour of the soft wheat variety Kadet. Methylation analysis

---

*Author for correspondence.

of the polysaccharide was performed[6] in dimethylsulfoxide using butyl-lithium (15% in hexane)[10] and methyl iodide.

N.m.r. spectroscopy. — Samples were exchanged three times with D_2O (99.9 atom% D, MSD Isotopes), finally using 99.96 atom% D at pD ≥ 7. [1]H-N.m.r. spectra (500 MHz) were recorded with a Bruker AM-500 spectrometer (Bijvoet Center, Department of NMR Spectroscopy) and a probe temperature of 67°. The ^{1}H chemical shifts were measured by reference to the H-1 signal of Ara[2c] (positioned at δ 5.222, being the δ value at 27°, relative to the signal of internal acetone at δ 2.225 at 27°)[7]. The ^{13}C chemical shifts were measured by reference to the signal of internal 1,4-dioxane (δ 67.40 at 67°).
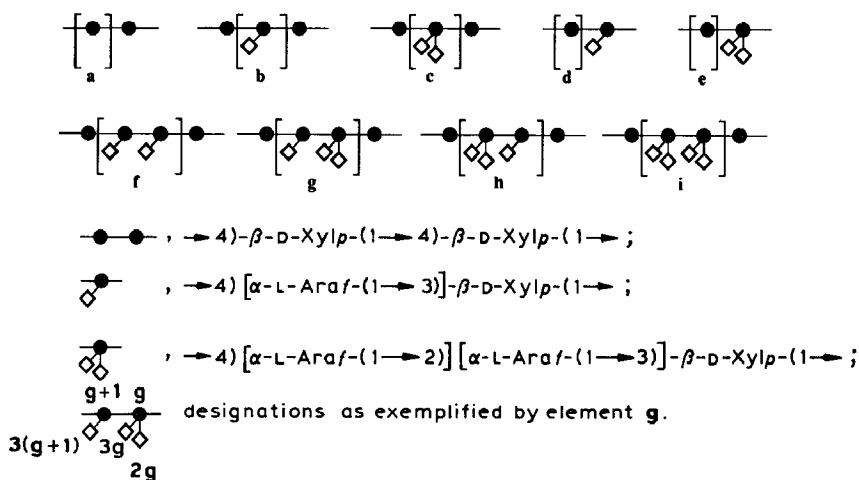
The 2D homonuclear Hartmann–Hahn (HOHAHA) spin-lock experiment on a 0.2% solution of the arabinoxylan involved the pulse sequence, $90°-t_1-SL-acq.$[11,12], where SL stands for a multiple of the MLEV-17 sequence. The spin-lock field strength corresponded to a 90° pulse width of 26 μs and a total spin-lock mixing time of 106 ms. The spectral width was 1500 Hz in each dimension. The proton-detected heteronuclear multiple-quantum correlation (HMQC)[13–15] spectrum of a 5% solution of the arabinoxylan involved the pulse sequence $90°([1]H)-1/[4J([1]H-[13]C)]-180°([1]H,[13]C)-1/[4J$ $([1]H-[13]C)]-90°([1]H,[13]C)-t_{1_2}-180°([1]H)-t_{1_2}-90°([13]C)-acq([1]H)$. No ^{13}C decoupling in the acquisition period was applied. The spectral width was 2500 Hz in the ω_2 dimension and 5682 Hz in the ω_1 dimension; 512 f.i.d.'s of 2K data points each were recorded for both the HOHAHA and HMQC experiment, and TPPI[16] was used to create t_1 amplitude modulation. Each data matrix was zero-filled to 1K × 4K and multiplied in the ω_2 time domain with a $\pi/4$, and in the ω_1 time domain with a $\pi/4$ (HOHAHA) or $\pi/2$ (HMQC), phase-shifted sine function prior to phase-sensitive F.t.

The natural-abundance proton-decoupled 1D ^{13}C-n.m.r. spectrum (75 MHz) of a 5% solution of the arabinoxylan in D_2O at 70° was recorded[6] with a Bruker MSL-300 spectrometer.

RESULTS AND DISCUSSION

Wheat arabinoxylans consist of a $(1\rightarrow4)$-β-D-Xyl*p* backbone, with the Xyl*p* residues variously unsubstituted, and 3- and 2,3-substituted with single α-L-Ara*f* groups. In the arabinoxylan studied, the ratios of these Xyl*p* residues were 39.9:6.7:10.4, as determined by methylation analysis[6]. The presence of relatively large quantities of 2,3-substituted Xyl*p* residues, and sufficient unsubstituted Xyl*p* residues to expect low proportions of highly clustered regions, made this polysaccharide attractive for the present investigation. The different types of elements found in arabinoxylan oligo-saccharides and characterised by [1]H-n.m.r. spectroscopy[8,9] are given in Scheme 1. Specific assignment of the α-Ara*f* H-5*proR*,5*proS* signals was based on their relative chemical shifts $(\delta_{5proR} > \delta_{5proS})$[17].

Fig. 1 shows the 1D [1]H-n.m.r. spectrum and Fig. 2 the 2D HOHAHA spectrum of the arabinoxylan, and the assignments are compiled in Table I. In order to facilitate the assignments of the H-2–H-5 signals, 1D subspectra of the different H-1 HOHAHA tracks were recorded. The line broadening of the [1]H-n.m.r. signals, caused by the high

Scheme 1 (structural diagrams a–i):

$\bullet\!-\!\bullet$, $-\!4)\text{-}\beta\text{-}D\text{-}Xyl p\text{-}(1\!-\!4)\text{-}\beta\text{-}D\text{-}Xyl p\text{-}(1\!-\!$;

, $-\!4)\,[\alpha\text{-}L\text{-}Ara f\text{-}(1\!-\!3)]\text{-}\beta\text{-}D\text{-}Xyl p\text{-}(1\!-\!$;

, $-\!4)\,[\alpha\text{-}L\text{-}Ara f\text{-}(1\!-\!2)]\,[\alpha\text{-}L\text{-}Ara f\text{-}(1\!-\!3)]\text{-}\beta\text{-}D\text{-}Xyl p\text{-}(1\!-\!$;

designations as exemplified by element g.

g+1 g

3(g+1) 3g

2g

Scheme 1.

α-Araf   β-Xylp

2[c,g,(h+1),i]

3[c,g,(h+1)]

3[b,f,(f+1)]

[f+1,g+1]   a   [d,e]

[c,g]   i

i+1   (1)   [b,f]

3i   3(i+1)

2(i+1)

(3)   3h   3(g+1)

(2)

h+1   h

×2

5.4   5.3   5.2   4.6   4.5

δ(p.p.m.)   δ(p.p.m.)

HOD

5.4   5.2   4.6   4.4   4.2   4.0   3.8   3.6   3.4   3.2
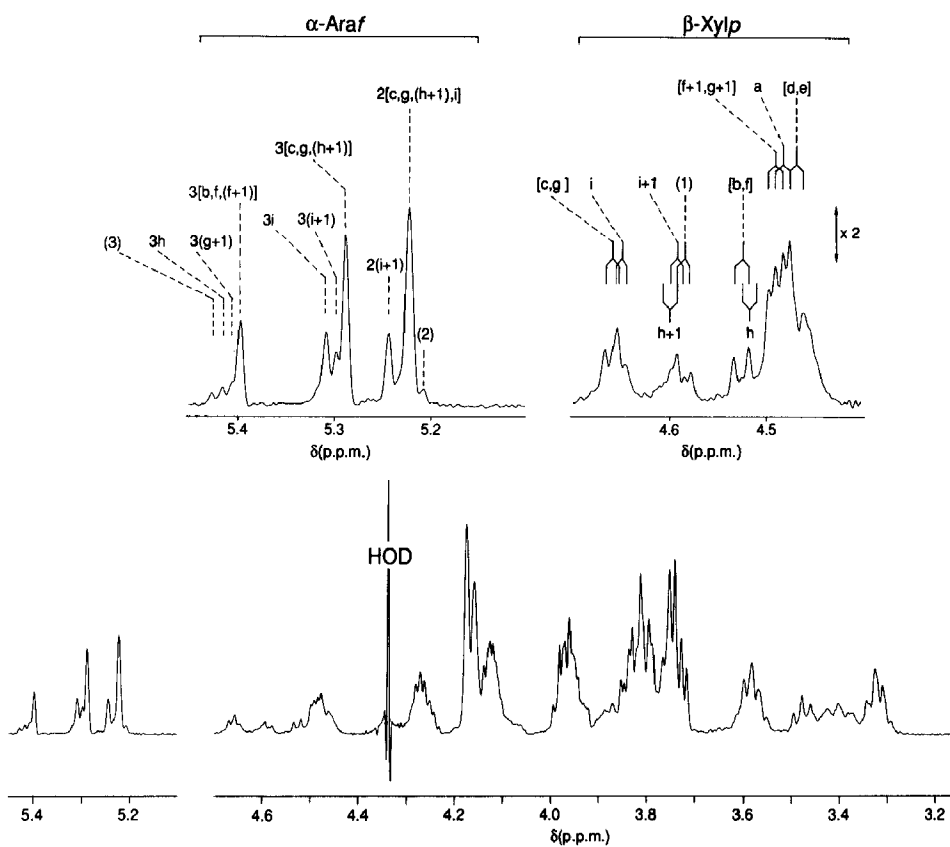
δ(p.p.m.)

Fig. 1. Resolution-enhanced 500-MHz ^{1}H-n.m.r. spectrum of a cold-water-soluble wheat-endosperm arabinoxylan at 67°, obtained from the first HOHAHA f.i.d., together with the expanded regions for the H-1 resonances. The codes in the spectrum refer to the corresponding residues in Scheme 1 (see also Table I).
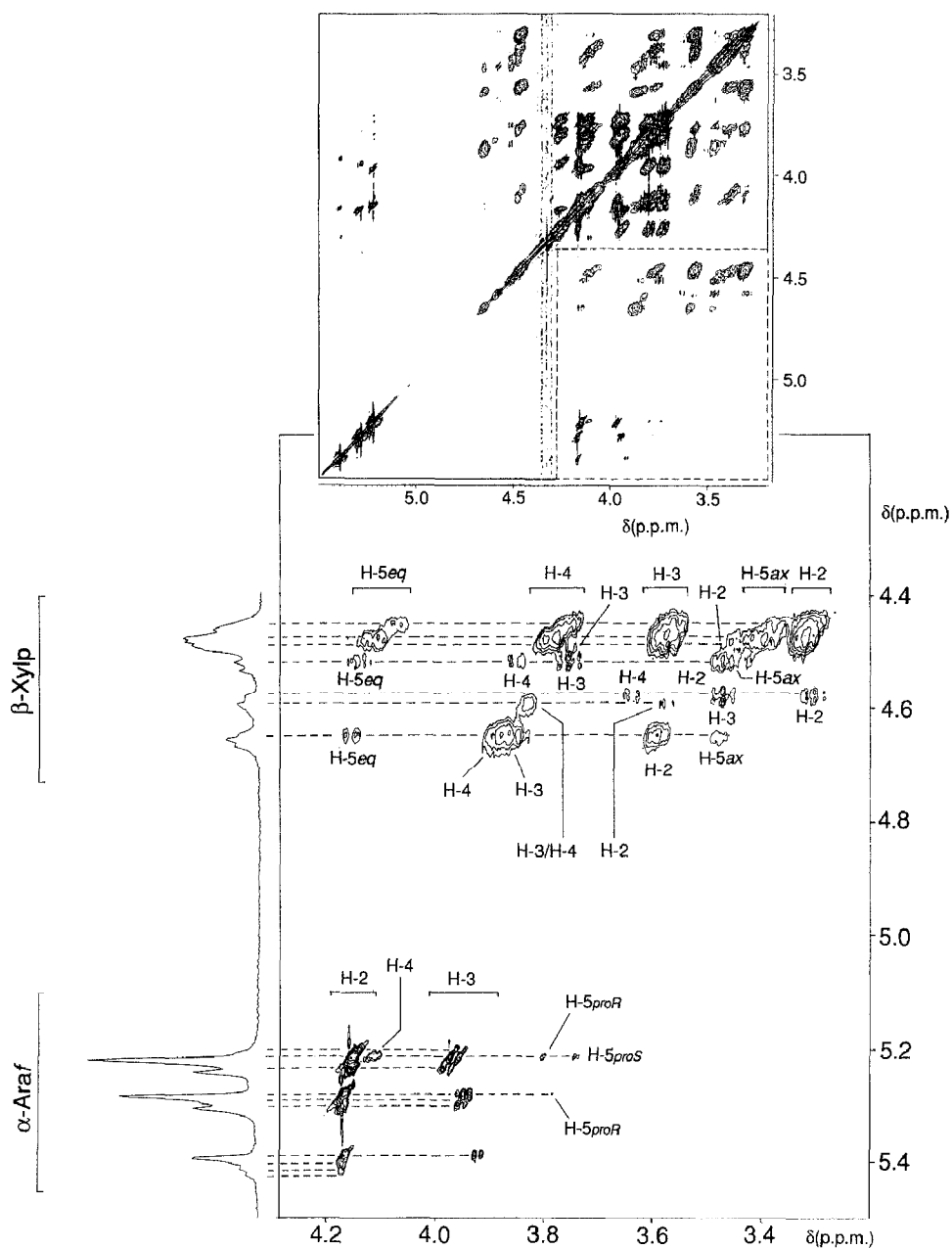
Fig. 2. HOHAHA spectrum of a cold-water-soluble wheat-endosperm arabinoxylan at 67°. A selected region, showing the skeleton-proton resonances along the H-1 tracks, is enlarged and lines are drawn to show scalar coupled networks. The 1D ^{1}H-n.m.r. spectrum of the region of H-1 resonances is included along the ω_1-axis.

TABLE I

^{1}H-N.m.r. data for the constituent monosaccharides present in the various elements (Scheme 1) of the cold-water-soluble L-arabino-D-xylan from the soft wheat variety Kadet, measured at 67°

Compound[a]	Chemical shift[b]					
	H-1	H-2	H-3	H-4	H-5eq/5proR	H-5ax/5proS
β-Xylp						
Xyl[a]	4.483	3.32	3.58	3.79	4.12	3.40
Xyl[b,f]	4.526	3.47	3.76	3.86	4.14	3.43
Xyl[c,g]	4.661					
		3.59	3.87	3.88	4.16	3.47
Xyl[i]	4.652					
Xyl[d,e]	4.46	3.31	3.56	3.75	4.07	3.36
Xyl[i+1]	4.590					
		3.58	3.83			
Xyl[h+1]	4.600					
Xyl[h]	4.518					
Xyl[f+1,g+1]	4.489	3.44	3.74			
Xyl-(1)	4.585	3.31	3.47	3.64		
α-Araf						
Ara[2c,2g,2(h+1),2i]	5.222	4.16	3.97	4.12	3.82	3.73
Ara[2(i+1)]	5.243	4.16	3.98			
Ara-(2)	5.207	4.15	3.96			
Ara[3c,3g,3(h+1)]	5.287	4.17	3.95	4.26	3.79	3.73
Ara[3(i+1)]	5.298	4.17	3.95			
Ara[3i]	5.308	4.17	3.96			
Ara[3b,3f,3(f+1)]	5.396					
		4.17	3.93	4.24	3.80	3.72
[c]Ara[3(g+1)]	5.406					
Ara[3h]	5.415	4.18	3.94			
Ara-(3)	5.426	4.18				

[a]Xyl[f], first β-Xylp residue of element f, counted from the right side (see Scheme 1); Xyl[f+1], second β-Xylp residue of element f; Ara[3f], α-Araf bound to O-3 of Xyl[f], etc. [b]In p.p.m. relative to the signal of Ara[2c] H-1, resonating at δ 5.222 in D$_2$O at 27° (ref. 7) (internal acetone, δ 2.225), acquired at 500 MHz. [c]Tentative assignment.

viscosity of the solution, was reduced by recording the spectra at 67°, but relaxation differences between the anomeric signals of α-Araf and β-Xylp remained.

As is evident from Figs. 1 and 2 and Table I, the elements **b** (Xyl[b] and Ara[3b]) and **c** (Xyl[c], Ara[2c], and Ara[3c]), together with their contiguous unbranched β-Xylp elements **d** (Xyl[d]) and **e** (Xyl[e]), are major constituents of the arabinoxylan. The differences in chemical shifts between the ^{1}H signals of β-Xylp in elements **d** and **e**, as shown for oligosaccharides[8], were too small to give separate signals, and the mean values are included (Xyl[d,e]). An unbranched β-Xylp residue linked to another unbranched β-Xylp residue, as in element **a** (Xyl[a]), was identified by the ^{1}H chemical shift data[8] (Table I). Besides the major elements **a–e**, minor elements were present. The element **i** was present, as followed from the signals of the two 2,3-branched β-Xylp (Xyl[i] and Xyl[i+1]) and of the

four α-Araf residues [Ara^{2i}, Ara^{3i}, Ara$^{2(i+1)}$, and Ara$^{3(i+1)}$]. The H-1 signals of Ara^{3i}, Ara$^{2(i+1)}$, and Ara$^{3(i+1)}$ had typical chemical shifts[9]. The H-2,3 signals along the H-1 track at δ 4.489 (Fig. 2, Table I) indicated the presence of Xyl^{f+1} (element f) and/or Xyl^{g+1} (element g). The structures of elements f and g were different, but both the Araf and Xylp signals that were derived from [Ara^{3f}]–Xyl^f and [Ara^{2g}][Ara^{3g}]–Xyl^g resonated at positions the same as those of elements b and c, respectively. The spectral differences between the elements f and g stemmed probably from the Ara$^{3(f+1)}$ and Ara$^{3(g+1)}$ H-1 resonances. However, the signals of Ara$^{3(f+1)}$ had approximately the same chemical shifts as those of the resonances of Ara^{3b} and Ara^{3f}. The presence of element h in the arabinoxylan was supported by the specific Ara^{3h} H-1 (δ 5.415) and Xyl^{h+1} H-1 (δ 4.600) signals. The intensities of the H-1 signal of each residue indicated that element h was present only in a low proportion consistent with earlier observations[9]. Only in the 1D ^{1}H-n.m.r. spectrum could the H-1 signal of Xyl^h (δ 4.518) be observed. The resonances of the Ara^{2h+1} and Ara^{3h+1} protons had approximately the same chemical shifts as those of the resonances of Ara^{2c} and Ara^{3c}, respectively. The H-1 signals of the elements given in Scheme 1 accounted for the greater part of the ^{1}H-n.m.r. spectrum. However, the H-1 signals designated in Table I as Xyl-(1) and Ara-(2),(3) have not yet been assigned. Presumably, they are derived from residues of structures having three contiguous branched residues, but no suitable reference ^{1}H-n.m.r. data are available.

The ^{1}H-n.m.r. chemical shift data of the arabinoxylan were correlated with ^{13}C-n.m.r. chemical shifts (Fig. 3A), via a 2D HMQC n.m.r. experiment (Fig. 3B), and the major ^{13}C signals could be assigned (Table II). Because no ^{13}C decoupling was

TABLE II

^{13}C-N.m.r. data for the cold-water-soluble L-arabino-D-xylan from the soft wheat variety Kadet, measured at 67°; only the major elements a, b, c, d, and e are assigned

Residue[a]	Chemical shift[b]				
	C-1	C-2	C-3	C-4	C-5
Element a					
Xyl^a	102.49	73.56	74.64	77.29	63.85
Element b					
Xyl^b	102.43	74.37	78.38	78.13	63.59
Ara^{3b}	108.45	81.69	78.13	85.60	62.31
Element c					
Xyl^c	100.81	74.64	78.13	78.13[c]	63.21
Ara^{2c}	109.47	82.30	77.70	85.09	62.18
Ara^{3c}	108.83	81.96	78.13	85.30	62.18
Element d,e					
Xyl^{d,e}	102.09	73.84	74.64	77.29[c]	63.85

[a]See Scheme 1 and Table I. [b]In p.p.m. relative to the signal of internal 1,4-dioxane at δ 67.40 in D$_2$O at 67°. [c]Tentative assignment.
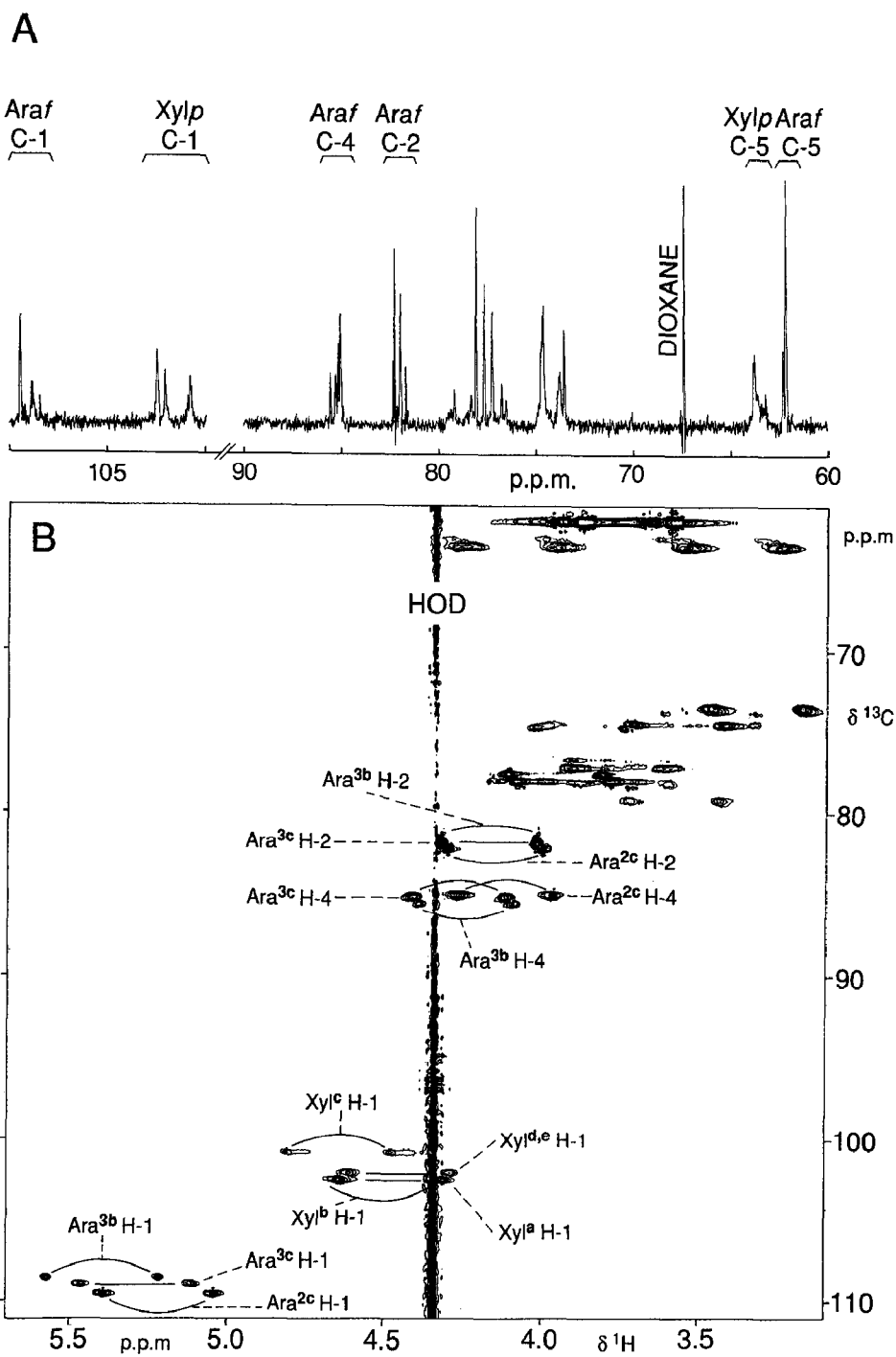
Fig. 3. Resolution-enhanced 75-MHz ^{13}C-n.m.r. spectrum (A) and 500-MHz ^{13}C-^{1}H HMQC spectrum (B) of a cold-water-soluble wheat-endosperm arabinoxylan at 70° and 67°, respectively.

applied during the acquisition period, each ^{1}H signal was split into two anti-phase signals by the ^{1}H–^{13}C coupling. The C-1 signal at δ 102.09 originated from Xyl^{d,e}, given by the upfield H-1 signal, and not from Xyl^b, as reported[18]. The C-1 signal of Xyl^{b,f}, and presumably also the C-1 signals of Xyl^{f+1} and Xyl^{g+1}, resonated at δ 102.43. Along the C-1 track of Xyl^c (δ 100.81; Fig. 3B), the C-1 signals of Xyl^i, Xyl^{i+1}, and Xyl^{h+1} were also present. The broadening of the α-Araf signals on the three C-1 tracks in the ^{1}H-direction indicated that, whereas the chemical shifts of the H-1 resonances of identically linked Araf residues (e.g., Ara^{2i} and Ara$^{2(i+1)}$) were influenced by the presence of neighbouring branched Xylp residues (Figs. 1 and 2), the chemical shifts of the C-1 resonances were not. This finding means that the presence and, to a certain extent, the relative abundance of the branching types, i.e., unsubstituted, 3-substituted, and 2,3-substituted Xylp residues, could be deduced from the ^{13}C-n.m.r. spectrum, but not of units of contiguous, branched residues. As has been shown[6], not only the Araf C-1 signals but also the well-separated C-2 and C-4 signals can give information about the major branching types of the arabinoxylan structure.

The results show that n.m.r. spectroscopy can provide information about the pattern of branching in arabinoxylans. However, due to the heterogeneous distribution of the branches along the xylan backbone, only the presence of units of contiguous, and 3- and/or 2,3-branched xylose residues could be determined from the ^{1}H-n.m.r. data, and not their relative proportions. The ^{13}C-n.m.r. spectrum of the arabinoxylan was less complex, yet only the presence and, to a certain extent, the relative abundance of the different branching types (i.e., 3- and 2,3-) could be determined. In order to obtain quantitative data on the various branched units present, degradation by endo-xylanases and chromatographic techniques will have to be used.

REFERENCES

1   H. J. Moss and N. L. Stenvert, Aust. J. Agric. Res., 22 (1971) 547–551.
2   R. P. C. Tao and Y. Pomeranz, J. Food Sci., 32 (1967) 162–168.
3   R. R. Mod, F. L. Normand, R. L. Ory, and E. J. Conkerton, J. Food Sci., 46 (1981) 571–573.
4   M. C. Kühn and W. Grosch, Cereal Chem., 66 (1989) 149–154.
5   G. O. Aspinall and K. M. Ross, J. Chem. Soc., (1963) 1681–1686.
6   R. A. Hoffmann, M. Roza, J. Maat, J. P. Kamerling, and J. F. G. Vliegenthart, Carbohydr. Polym., 15 (1991) 415–430.
7   R. A. Hoffmann, M. Roza, J. Maat, J. P. Kamerling, and J. F. G. Vliegenthart, Carbohydr. Polym., 16 (1991) 275–289.
8   R. A. Hoffmann, B. R. Leeflang, M. M. J. de Barse, J. P. Kamerling, and J. F. G. Vliegenthart, Carbohydr. Res., 221 (1991) 63–81.
9   R. A. Hoffmann, T. Geijtenbeek, J. P. Kamerling, and J. F. G. Vliegenthart, Carbohydr. Res., 223 (1992) 19–44.
10 A. L. Kvernheim, Acta Chem. Scand., Ser. B, 41 (1987) 150–152.

11 A. Bax and D. G. Davis, *J. Magn. Reson.*, 65 (1985) 355–360.
12 M. W. Edwards and A. Bax, *J. Am. Chem. Soc.*, 108 (1986) 918–923.
13 L. Müller, *J. Am. Chem. Soc.*, 101 (1979) 4481–4484.
14 D. Brühwiler and G. Wagner, *J. Magn. Reson.*, 69 (1986) 546–551.
15 G. Otting and K. Wüthrich, *J. Magn. Reson.*, 76 (1988) 569–574.
16 D. Marion and K. Wüthrich, *Biochem. Biophys. Res. Commun.*, 113 (1983) 967–974.
17 G. D. Wu, A. S. Serianni, and R. Baker, *J. Org. Chem.*, 48 (1983) 1750–1757.
18 S. Bengtsson and P. Åman, *Carbohydr. Polym.*, 12 (1990) 267–277.